PHYSICAL REVIEW C **74**, 062201(R) (2006)

Nuclear transparencies from photoinduced pion production

W. Cosyn,* M. C. Martínez,† J. Ryckebusch, and B. Van Overmeire
Department of Subatomic and Radiation Physics, Ghent University, Proeftuinstraat 86, B-9000 Gent, Belgium
(Received 25 July 2006; revised manuscript received 12 October 2006; published 21 December 2006)

We present a relativistic and cross-section factorized framework for computing nuclear transparencies extracted from $A(\gamma, \pi N)$ reactions at intermediate energies. The proposed quantum mechanical model adopts a relativistic extension to the multiple-scattering Glauber approximation to account for the final state interactions of the ejected nucleon and pion. The theoretical predictions are compared against the experimental $^4\text{He}(\gamma, p\pi^-)$ data from the Thomas Jefferson National Accelerator Facility. For those data, our results show no conclusive evidence of the onset of mechanisms related to color transparency.

DOI: 10.1103/PhysRevC.74.062201 PACS number(s): 25.20.Lj, 21.60.Cs, 24.10.Jv, 25.10.+s

The strong interaction exhibits a strong scale dependence. At low energies, hadrons are undoubtedly the adequate degrees of freedom. The properties of nuclei can be fairly well understood in a picture in which nucleons exchange mesons. At high energies, that particular role of fermions interacting through force-carrying bosons is played by quarks and gluons. The transition energy region is a topic of current intensive research at, for example, the Thomas Jefferson National Accelerator Facility (Jefferson Lab), where hadronic matter can be studied with intense beams of real and virtual photons possessing the proper wavelengths in the femtometer and subfemtometer range. An observable commonly used to pin down the underlying dynamics of hadronic matter is the nuclear transparency to the transmission of hadrons. The nuclear transparency for a certain reaction process is defined as the ratio of the cross section per target nucleon to the one for a free nucleon. Accordingly, the transparency is a measure of the effect of the medium on the passage of energetic hadrons. It provides an excellent tool for searching for deviations from predictions of models based on traditional nuclear physics. One such phenomenon is color transparency (CT). Color transparency predicts the reduction of final state interactions (FSI) of hadrons propagating through nuclear matter in processes at high momentum transfer. Experiments have been carried out to measure nuclear transparencies in search of CT in $A(p, 2p)$ [1–4] and $A(e, e'p)$ [5–10] reactions, ρ-meson production [11,12], and diffractive dissociation of pions into di-jets [13]. Intuitively, one expects CT to reveal itself more rapidly in reactions involving mesons. Indeed, it appears to be more probable to produce a two-quark configuration with a small transverse size and, as a consequence, reduced FSI.

Recently, the nuclear transparency for the pion photoproduction process $\gamma n \rightarrow \pi^- p$ in ^{4}He has been measured in Hall A at Jefferson Lab [14]. In the experiment, both the outgoing proton and the pion are detected for photon beam energies in the range 1.6–4.5 GeV and pion center-of-mass scattering angles of 70° and 90°. With two hadrons in the final state, the pion photoproduction reaction on helium offers good opportunities for searching for medium effects that go beyond traditional nuclear physics. Not only is He a dense system, but also its small radius optimizes the ratio of the hadron formation length to the size of the system. Along the same line, a pion electroproduction experiment at Jefferson Lab measuring pion transparencies in H, D, ^{12}C, ^{64}Cu, and ^{197}Au [15] has been completed, and data analysis is currently under way. It speaks for itself, though, that the availability of a model for computing transparencies extracted from $A(\gamma, \pi N)$ and $A(e, e'\pi N)$ is essential for interpreting all these measurements. As a matter of fact, it is a real challenge to compute the effect of the medium on the simultaneous emission of a nucleon and a pion within the context of traditional nuclear physics models.

In Ref. [14], the results for $\gamma n \rightarrow \pi^- p$ on ^{4}He are compared to the predictions of a semiclassical model by Gao, Holt, and Pandharipande [16]. The results of the calculations including CT effects were found to be more consistent with the measurements. An alternative semiclassical approximation to compute pionic transparencies is presented in Ref. [17]. A quantum mechanical model for meson photoproduction on ^{2}H was recently proposed by J. M. Laget [18]. In this Rapid Communication, we present a quantum mechanical model for computing the nuclear transparencies in $\gamma n \longrightarrow \pi^- p$ on finite nuclei. The model is based on a relativized version of Glauber theory and is essentially parameter free. To our knowledge, the presented framework is the first of its kind.

In describing the $A(\gamma, N\pi)A-1$ reaction, we use the following laboratory four-momenta: $Q^\mu(q, \vec{q})$ for the photon, $P_A^\mu(E_A, \vec{p}_A = \vec{O})$ for the target nucleus, $P_{A-1}^\mu(E_{A-1}, \vec{p}_{A-1})$ for the residual nucleus, and $P_N^\mu = (E_N, \vec{p}_N)$ and $P_\pi^\mu = (E_\pi, \vec{p}_\pi)$ for the ejected nucleon and pion. The missing momentum $\vec{p}_m$ is defined as $\vec{p}_m = -\vec{p}_{A-1} = \vec{p}_N + \vec{p}_\pi - \vec{q}$. Following the conventions of Ref. [19], the fivefold differential cross section reads in the laboratory frame

$$\frac{d\sigma}{dE_\pi d\Omega_\pi d\Omega_N} = \frac{M_{A-1} m_N p_\pi p_N}{4(2\pi)^5 q E_A} f_{\text{rec}}^{-1} \overline{\sum_{if}} \left| \mathcal{M}_{fi}^{(\gamma, N\pi)} \right|^2, \quad (1)$$

with the recoil factor given by

$$f_{\text{rec}} = \frac{E_{A-1}}{E_A} \left| 1 + \frac{E_N}{E_{A-1}} \left(1 + \frac{(\vec{p}_\pi - \vec{q}) \cdot \vec{p}_N}{p_N^2} \right) \right|, \quad (2)$$

*Electronic address: Wim.Cosyn@UGent.be
†Present address: Dpto FAMN, Universidad Complutense de Madrid, E-28040 Madrid, Spain.

and $\mathcal{M}_{fi}^{(\gamma,N\pi)}$ is the invariant matrix element

$$\mathcal{M}_{fi}^{(\gamma,N\pi)} = \left\langle P_\pi^\mu, P_N^\mu m_s, P_{A-1}^\mu J_R M_R \middle| \hat{\mathcal{O}} \middle| Q^\mu, P_A^\mu 0^+ \right\rangle, \quad (3)$$

where m_s is the spin of the ejected nucleon N, and $J_R M_R$ the quantum numbers of the residual nucleus. We restrict ourselves to processes with an even-even target nucleus A. The operator $\hat{\mathcal{O}}$ describes the pion photoproduction process, and we assume it to be free from medium effects. This is a common assumption in nuclear and hadronic physics and is usually referred to as the impulse approximation (IA).

For the target and residual nucleus, we use relativistic wave functions as they are obtained in the Hartree approximation to the $\sigma\omega$ model with the W1 parametrization [20]. When studying the transparency, it is convenient to factorize the invariant matrix element $\mathcal{M}_{fi}^{(\gamma,N\pi)}$ into a part containing the elementary pion photoproduction process and a part with the typical medium mechanisms in the process under study. It is clear that the attenuation on the ejected proton and pion induced by FSI mechanisms belongs to the last category and determines the nuclear transparency for the process under study. Even in the relativistic plane-wave limit for the ejected nucleon and pion wave function, factorization of the cross section is not reached through the presence of negative-energy contributions. Neglecting these, the computation leads to an expression for the cross section in the relativistic plane wave impulse approximation (RPWIA) that reads

$$\left(\frac{d\sigma}{dE_\pi d\Omega_\pi d\Omega_N}\right)_{\text{RPWIA}} \approx \frac{M_{A-1} p_\pi p_N (s-(m_N)^2)^2}{4\pi m_N q M_A} f_{\text{rec}}^{-1} \rho^\alpha(\vec{p}_m) \frac{d\sigma^{\gamma\pi}}{d|t|}, \quad (4)$$

with $\rho^\alpha(\vec{p}_m) = \sum_{m_s,m} |\bar{u}(\vec{p}_m, m_s)\phi_\alpha(\vec{p}_m)|^2$ the momentum distribution obtained by contracting the bound-state wave function ϕ_α with the Dirac spinor $\bar{u}$. The $\alpha(n,\kappa,m)$ denotes the quantum numbers of the bound nucleon on which the photon is absorbed. Further, $\frac{d\sigma^{\gamma\pi}}{d|t|}$ denotes the cross section for $\gamma + N \longrightarrow \pi + N'$, and $s = (Q^\mu + P_A^\mu)^2$ and $t = (Q^\mu - P_\pi^\mu)^2$ are the Mandelstam variables.

In this work, we concentrate on $A(\gamma, N\pi)A-1$ processes for which the wavelengths of the ejected nucleons and pions are typically smaller than their interaction ranges with the nucleons in the rest nucleus. Those conditions make it possible to describe the FSI mechanisms with the aid of a Glauber model. A relativistic extension of the Glauber model, dubbed the relativistic multiple-scattering Glauber approximation (RMSGA), was introduced in Ref. [21]. In the RMSGA, the wave function for the ejected nucleon and pion is a convolution of a relativistic plane wave and an eikonal Glauber phase operator $\widehat{\mathcal{S}}_{\text{FSI}}(\vec{r})$ which accounts for all FSI mechanisms. Through the operation of $\widehat{\mathcal{S}}_{\text{FSI}}(\vec{r})$ every residual nucleon in the forward path of the outgoing pion and nucleon adds an extra phase to their wave function. The RMSGA framework has proved successful in describing cross sections and other observables in exclusive $A(e,e'p)$ [21,22] and $A(p,2p)$ [23] reactions. The numerically challenging component in RMSGA is that $\widehat{\mathcal{S}}_{\text{FSI}}(\vec{r})$ involves a multiple integral which tracks the effect of all collisions of an energetic nucleon and pion with the remaining nucleons in the target nucleus. Realistic nuclear wave functions are also used in the models of Refs. [16,17]. Contrary to the RMSGA model, however, the transparencies are computed at the squared amplitude level adopting a semiclassical picture for the FSI mechanisms.

In the numerical calculations within the context of the RMSGA, the following phase is added to the product wave function for the ejected nucleon and pion:

$$\widehat{\mathcal{S}}_{\text{FSI}}(\vec{r}) = \prod_{j=2}^{A} [1 - \Gamma_{N'N}(\vec{b} - \vec{b}_j)\theta(z_j - z)] \times [1 - \Gamma_{\pi N}(\vec{b}' - \vec{b}'_j)\theta(z'_j - z')], \quad (5)$$

where $\vec{r}_j(\vec{b}_j, z_j)$ are the coordinates of the residual nucleons, and $\vec{r}(\vec{b}, z)$ specifies the interaction point with the photon. In Eq. (5), the z and z' axes lie along the path of the ejected nucleon and pion, respectively. The $\vec{b}$ and $\vec{b}'$ are perpendicular to these paths. Reflecting the diffractive nature of the nucleon-nucleon ($N'N$) and pion-nucleon (πN) collisions at intermediate energies, the profile functions $\Gamma_{N'N}$ and $\Gamma_{\pi N}$ in Eq. (5) are parametrized as

$$\Gamma_{iN}(\vec{b}) = \frac{\sigma_{iN}^{\text{tot}}(1 - i\epsilon_{iN})}{4\pi\beta_{iN}^2} \exp\left(-\frac{\vec{b}^2}{2\beta_{iN}^2}\right) \quad (\text{with } i = \pi \text{ or } N') . \quad (6)$$

Here, the parameters σ_{iN}^{tot} (total cross section), β_{iN} (slope parameter), and ϵ_{iN} (real to imaginary part ratio of the amplitude) depend on the momentum of the outgoing particle i. In our calculations, those parameters are obtained by interpolating data from the databases for $N'N \longrightarrow N'N$ from the Particle Data Group [24] and $\pi N \longrightarrow \pi N$ from the analysis of Refs. [25,26].

Now we derive an expression for the fivefold $A(\gamma, N\pi)$ $A-1$ cross sections when implementing FSI effects. To this end, we define the distorted momentum distribution

$$\rho_{\text{RMSGA}}^\alpha(\vec{p}_m) = \sum_{m_s,m} |\bar{u}(\vec{p}_m, m_s)\phi_\alpha^D(\vec{p}_m)|^2 . \quad (7)$$

Here, $\phi_\alpha^D(\vec{p}) = \frac{1}{(2\pi)^{3/2}} \int d\vec{r} e^{-i\vec{p}\cdot\vec{r}} \phi_\alpha(\vec{r}) \widehat{\mathcal{S}}_{\text{FSI}}^\dagger(\vec{r})$ is the distorted momentum-space wave function, which is the Fourier transform of the bound nucleon wave function and the total Glauber phase. In the absence of FSI, the $\rho_{\text{RMSGA}}^\alpha(\vec{p}_m)$ of Eq. (7) reduces to the $\rho^\alpha(\vec{p}_m)$ in Eq. (4) when negative-energy components are neglected. Based on this analogy, we obtain the cross section in the RMSGA approach by replacing $\rho^\alpha(\vec{p}_m)$ by $\rho_{\text{RMSGA}}^\alpha(\vec{p}_m)$ in Eq. (4).

In our calculations, color transparency effects are implemented in the standard fashion by replacing the total cross sections σ_{iN}^{tot} in Eq. (6) with effective ones [27] which account for some reduced interaction over a typical length scale l_h corresponding with the hadron formation length ($i = \pi$ or N'), that is,

$$\frac{\sigma_{iN}^{\text{eff}}}{\sigma_{iN}^{\text{tot}}} = \left\{ \left[\frac{\mathcal{Z}}{l_h} + \frac{\langle n^2 k_t^2 \rangle}{t} \left(1 - \frac{\mathcal{Z}}{l_h}\right) \theta(l_h - \mathcal{Z}) \right] + \theta(\mathcal{Z} - l_h) \right\} . \quad (8)$$

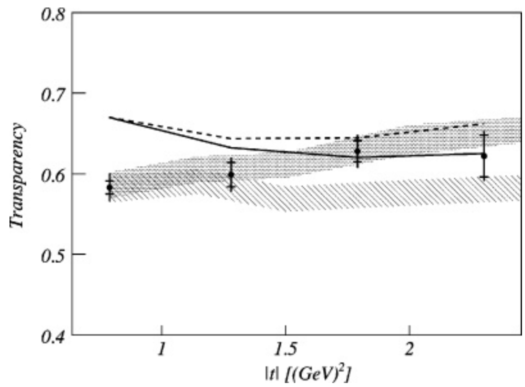

FIG. 1. Nuclear transparency extracted from ^{4}He(γ, $p\pi^-$) vs squared momentum transfer $|t|$ at $\theta^{\pi}_{\mathrm{c.m.}} = 70°$. Solid (dashed) curve is the result of the RMSGA calculations without (with) color transparency. Semiclassical model [16] results are presented by the shaded areas: hatched (dotted) area is a calculation without (with) CT. Data from Ref. [14].

Here n is the number of elementary fields (2 for the pion, 3 for the nucleon), $k_t = 0.350$ GeV/c is the average transverse momentum of a quark inside a hadron, $\mathcal{Z}$ is the distance the object has traveled since its creation, and $l_h \simeq 2p/\Delta M^2$ is the hadronic expansion length, with p the momentum of the final hadron and ΔM^2 the mass squared difference between the intermediate prehadron and the final hadron state. We adopted the values $\Delta M^2 = 1\,\mathrm{GeV}^2$ for the proton and $\Delta M^2 = 0.7\,\mathrm{GeV}^2$ for the pion.

In Figs. 1 and 2, we present the results of transparency calculations for ^{4}He together with the experimental data and the predictions of the semiclassical model of Ref. [16]. In comparing transparency measurements with theory, accurate modeling of the experimental cuts is required. We adopt the following definition for the transparency

$$T = \frac{\sum_i \sum_\alpha Y(q_i) \left(\frac{d\sigma}{dE_{\pi_i} d\Omega_{\pi_i} d\Omega_{N_i}} \right)_{\mathrm{RMSGA}}}{\sum_i \sum_\alpha Y(q_i) \left(\frac{d\sigma}{dE_{\pi_i} d\Omega_{\pi_i} d\Omega_{N_i}} \right)_{\mathrm{RPWIA}}}, \qquad (9)$$

where i denotes an event within the ranges set by the detector acceptances and applied cuts. Further, $\sum_\alpha$ extends over all occupied single-particle states in the target nucleus. All cross sections are computed in the laboratory frame. Further, $Y(q)$ is the yield of the reconstructed experimental photon beam spectrum for a certain photon energy [14]. We assume that the elementary $\gamma + n \rightarrow \pi^- + p$ cross section $\frac{d\sigma^{\gamma\pi}}{d|t|}$ in Eq. (4) remains constant over the kinematic ranges which define a particular data point. With this assumption, the cross section $\frac{d\sigma^{\gamma\pi}}{d|t|}$ cancels out of the ratio (9). In order to reach convergence in the phase-space averaging $\sum_i$ in Eq. (9), we generated about one thousand theoretical events within the kinematic ranges of the experimental acceptances. This was done for all data points, eight in total, and corresponding kinematic ranges, of the Jefferson Lab experiment. Detailed kinematics for these data points can be found in Ref. [14].

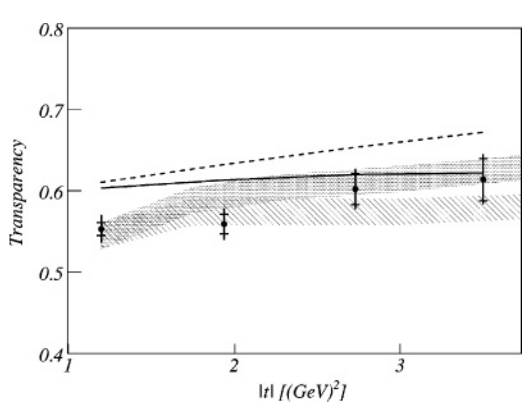

FIG. 2. As in Fig. 1, but for $\theta^{\pi}_{\mathrm{c.m.}} = 90°$.

The computed RMSGA nuclear transparencies are systematically about 10% larger than those obtained in the semiclassical model. As can be seen in Fig. 1, our model predicts a rise in the transparency for $|t|$ values below $1.2\,\mathrm{GeV}^2$. This rise is due to the minimum in the total proton-nucleon cross section in Eq. (6) for the proton momenta associated with these momentum transfers. The RMSGA results overestimate the measured transparencies at small $|t|$, but do reasonably well for the higher values of $|t|$. Inclusion of CT effects tends to increase the predicted transparency at a rate which depends on a hard-scale parameter. Here, that role is played by the momentum transfer $|t|$. Thus, inclusion of CT mechanisms results in an increase of the nuclear transparency which grows with the momentum transfer $|t|$. The magnitude of the increase depends on the choice of the parameters in Eq. (8). For the moment, there are no experimental constraints on their magnitude. As can be appreciated from Figs. 1 and 2, the RMSGA calculations predict CT effects comparable to those from the semiclassical calculations. We have to stress, though, that the calculations with CT are normalized to the calculations without CT for the data point with the lowest $|t|$ in the semiclassical model. We did not perform this normalization for our calculations. Our results without color transparency are in better agreement with the experimental results than those with CT effects included. This result is contrary to that with the semiclassical model, whose results with CT effects are in better agreement with the experimental data. We also have to point out that although the calculations with CT effects overestimate the experimental results for all data points, the

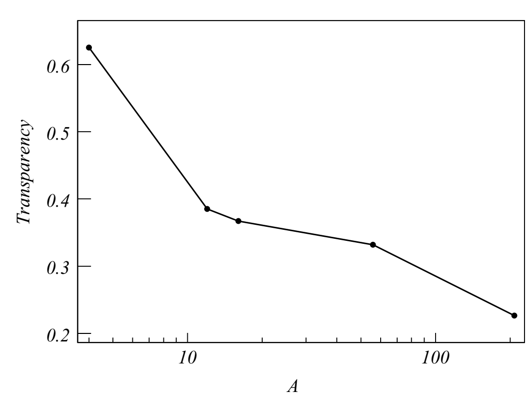

FIG. 3. A dependence of the transparency. Calculations were made for ^{4}He, ^{12}C, ^{16}O, ^{56}Fe, and ^{208}Pb at $|t| = 3.5\,\mathrm{GeV}^2$ for $\theta^{\pi}_{\mathrm{c.m.}} = 90°$ without color transparency.

slope of this curve shows better agreement with the slope of the data than does the slope of the curves without CT effects.

To provide an idea of the A dependence of the nuclear transparency extracted from $A(\gamma, p\pi^-)$, we plotted in Fig. 3 the calculations for one data point for several nuclei with the same kinematic cuts as before. However, because of these cuts, nucleon knockout from the innermost shells in the heavier nuclei was not always possible for the generated events in the calculations. The transparency would be even lower for these heavier nuclei if no cuts were to be applied.

In summary, we have developed a quantum mechanical model based on a relativistic extension to multiple-scattering Glauber theory to calculate nuclear transparencies extracted from $A(\gamma, N\pi)$ processes. The model can be applied to any even-even target nucleus with a mass number $A \geqslant 4$. The nuclear transparency is the result of the attenuating effect of the medium on the ejected proton and pion, and it is computed by means of a Glauber phase operator. The numerical computation of the latter requires knowledge about $\pi N \to \pi N$ and $N'N \to N'N$ cross sections, as well as a set of relativistic mean-field wave functions for the residual nucleus. In contrast to alternative models, which adopt a semiclassical approach, we treat FSI mechanisms at the amplitude level in a quantum mechanical and relativistic manner. Comparison with experimental results for helium shows no evidence of color transparency in our model. Further progress will very much depend on the availability of new data. The model presented here can be readily extended to electroproduction processes for comparison with the forthcoming Jefferson Lab data.

We are grateful to D. Dutta for useful discussions. This work is supported by the Fund for Scientific Research Flanders and the Research Board of Ghent University. M.C.M. acknowledges postdoctoral financial support from the Ministerio de Educación y Ciencia (MEC) of Spain.

[1] A. S. Carroll *et al*., Phys. Rev. Lett. **61**, 1698 (1988).
[2] I. Mardor *et al*., Phys. Rev. Lett. **81**, 5085 (1998).
[3] A. Leksanov *et al*., Phys. Rev. Lett. **87**, 212301 (2001).
[4] J. L. S. Aclander *et al*., Phys. Rev. C **70**, 015208 (2004).
[5] G. Garino *et al*., Phys. Rev. C **45**, 780 (1992).
[6] N. Makins *et al*., Phys. Rev. Lett. **72**, 1986 (1994).
[7] T. G. O'Neill *et al*., Phys. Lett. **B351**, 87 (1995).
[8] D. Abbott *et al*., Phys. Rev. Lett. **80**, 5072 (1998).
[9] K. Garrow *et al*., Phys. Rev. C **66**, 044613 (2002).
[10] D. Dutta (Jefferson Lab E91013 Collaboration), Phys. Rev. C **68**, 064603 (2003).
[11] M. R. Adams *et al*. (E665 Collaboration), Phys. Rev. Lett. **74**, 1525 (1995).
[12] A. Airapetian *et al*. (HERMES Collaboration), Phys. Rev. Lett. **90**, 052501 (2003).
[13] E. M. Aitala *et al*. (E791 Collaboration), Phys. Rev. Lett. **86**, 4773 (2001).
[14] D. Dutta *et al*. (Jefferson Lab E940104 Collaboration), Phys. Rev. C **68**, 021001 (2003).
[15] K. R. Garrow *et al*., JLAB-PR01-107 (unpublished).
[16] H. Gao, R. J. Holt, and V. R. Pandharipande, Phys. Rev. C **54**, 2779 (1996).
[17] A. Larson, G. A. Miller, and M. Strikman, Phys. Rev. C **74**, 018201 (2006).
[18] J. M. Laget, Phys. Rev. C **73**, 044003 (2006).
[19] J. D. Bjorken and S. D. Drell, *Relativistic Quantum Mechanics* (McGraw-Hill, New York, 1964).
[20] R. J. Furnstahl, B. D. Serot, and H.-B. Tang, Nucl. Phys. **A615**, 441 (1997).
[21] J. Ryckebusch, D. Debruyne, P. Lava, S. Janssen, B. Van Overmeire, and T. Van Cauteren, Nucl. Phys. **A728**, 226 (2003).
[22] P. Lava, M. C. Martinez, J. Ryckebusch, J. A. Caballero, and J. M. Udias, Phys. Lett. **B595**, 177 (2004).
[23] B. Van Overmeire, W. Cosyn, P. Lava, and J. Ryckebusch, Phys. Rev. C **73**, 064603 (2006).
[24] W.-M. Yao *et al*., J. Phys. G **33**, 1 (2006) and http://pdg.lbl.gov/
[25] R. A. Arndt, W. J. Briscoe, I. I. Strakovsky, R. L. Workman, and M. M. Pavan, Phys. Rev. C **69**, 035213 (2004).
[26] R. L. Workman (private communication).
[27] G. R. Farrar, H. Liu, L. L. Frankfurt, and M. I. Strikman, Phys. Rev. Lett. **61**, 686 (1988).